2	
3	Use of response surface methodology to develop and
4	optimize the composition of a chitosan-
5	polyethyleneimine-graphene oxide nanocomposite
6	membrane coating to more effectively remove
7	Cr(VI) and Cu(II) from water
8	
9	Pasan C. Bandara [†] , Enrico T. Nadres [†] , Debora F. Rodrigues ^{†*}
10	[†] Department of Civil and Environmental Engineering, University of Houston, Houston, TX
11	77204-4003. Email: dfrigirodrigues@uh.edu
12	
13	
14	
15	
16	
17 18	

ABSTRACT

1

Response surface methodology (RSM) was successfully used to optimize the amounts of chitosan 2 (CS), polyethyleneimine (PEI), graphene oxide (GO), and glutaraldehyde (GLA) to produce a 3 multifunctional nanocomposite membrane coating able to remove positively and negatively 4 charged heavy metals, such as Cr(VI) and Cu(II). Batch experiments with different concentrations 5 of the four coating components (GO, CS, PEI and GLA) on cellulose membranes were carried out 6 with solutions containing 10 ppm Cr(VI) and Cu(II) ions. Reduced quadratic equations for the 7 Cr(VI) and Cu(II) removals were obtained based on the observed results of the batch experiments. 8 9 The numerical analysis resulted in an optimized solution of 30-min soaking in CS, 1.95% PEI, 1000 ppm GO and 1.68% GLA with predicted removals of 90±10 % and 30±3% for Cr(VI) and 10 11 Cu(II), respectively, with a desirability of 0.99. This mathematically optimized solution for the coating was experimentally validated. To determine the best membrane material for the coating, 12 13 stability of the nanocomposite coating was determined using attenuated total reflectance - infrared 14 (ATR-IR) spectroscopy in eight membrane materials before and after exposure to four solutions with different water chemistries. The glass microfiber (GMF) membranes were determined to be 15 16 one of the best materials to receive the coating. Then, the coated GMF filter was further 17 investigated for the removal of Cr(VI) and Cu(II) in single and binary component solutions. 18 Results showed that the coatings were able to remove successfully both heavy metal ions, 19 suggesting its ability to remove positively and negatively charged ions from water.

20

21

22

Keywords: Chromium, Copper, graphene-oxide, nanocomposite, chitosan, water treatment, response surface methodology

23

1. INTRODUCTION

1

2

3

4

5

6

7

8

9

10

11

12

13

14

15

16

17

18

19

20

21

22

23

Recently, indirect potable reuse (IPR) has gained attention as an important sustainable water management process.¹ For communities with limited water resources available, IPR seems to be a promising water management option in terms of water sustainability. IPR can achieve high-quality recycled water in compliance with the drinking water standards. Recycling efforts, however, need to be completed with the continuous evaluation of the potential health effects of treated recycled water for drinking purposes, since based on the origin of the wastewater, it could still contain very low hazardous contaminant concentrations after treatment. ¹⁻³

One group of contaminants that can be hazardous even at low concentrations is heavy metals. Among the heavy metal removal techniques, there are electrodialysis⁴, coagulation, flotation⁵, activated carbon adsorption⁶, ion exchange, reverse osmosis, and chemical reduction and precipitation. From these, efficiency of the chemical precipitation technique depends on different factors, such as pH adjustment, flocculation, and the concentrations of the ions involved.⁸-⁹ Even though chemical precipitation is used widely, this technique requires chemicals and generate hazardous wastes. The other methods usually require long contact times. Thus, the production of potable water with the current methods can be expensive, and time-consuming. Therefore, it is important to search for alternative water treatment methods that are economical, efficient for the removal of different water contaminants. In search of such alternatives, many recent studies have shown potential use of nanotechnology and nanomaterials to remove numerous toxic contaminants efficiently and effectively from different contaminated water sources via adsorption. 10 Among other advantages, nanomaterials do not generate brines or other disinfectant byproducts during the adsorption processes and has been considered as an economically viable technology for wastewater and water treatment. 11

Graphene and its derivatives have been more recently widely investigated for water treatment purposes as they provide the potential for the modification or functionalization of its carbon backbone for better removal of contaminants. Graphene oxide (GO) is a chemically modified version of graphene that has been highlighted as a promising counterpart for diverse applications. GO has shown excellent antimicrobial properties against bacteria. In addition, GO can adsorb a vast range of cationic and anionic contaminants such as heavy metals and industrial cationic dyes. These removal capabilities are due to the physical properties of GO and the functional groups in GO such as -OH and -COOH, which can uptake positively and negatively charged particles via a process of chemical uptake and adsorption. On the such as a process of chemical uptake and adsorption.

Furthermore, GO is cost-effective and can be used in large-scale production of graphene-based materials or composites. 14, 22 Recently, the direction of research has moved toward incorporating such nanomaterials with polymeric substances to provide functional variety, structural strength, and stability. Research in the synthesis of nanocomposites for water treatment is favored by the fact that the properties of GO or graphene-based nanomaterials in general can be enhanced by the polymers. Adsorption capacity, selectivity, lowering life-cycle cost, improved design flexibility, and potential for large-scale fabrication are some of the advantages of incorporating GO into polymeric matrices. 23-24 In the present study, a combination of selected polymers with graphene oxide was used to develop and optimize a more efficient, effective, and multi-functional class of nanocomposite adsorbent for indirect potable water reuse treatment using the response surface methodology (RSM). RSM is considered as an effective method to understand the relationships between several independent variables and one or more response variables. The RSM was utilized in the present study for the optimization of the composite since it allows reduced number of experimental runs and easy control of factors. 21, 25 Furthermore, it has been extensively

- used in the experimental design and optimization processes of polymeric matrices where responses
 can be linked mathematically and statistically to the material composition.^{21, 25-26}
 - This study aims to find the optimum conditions to incorporate GO into a polymeric matrix composed by chitosan (CS) and polyethyleneimine (PEI), and crosslinked with glutaraldehyde (GLA). Compositions of GO and PEI, amounts of GLA and dip coating time in the CS solution were optimized based on two response variables, namely % Cr(VI) and % Cu(II) removals. An experimental matrix was generated based on an I-optimal design to establish the working region of the RSM. Obtained results were fitted into model equations in the form of quadratic equations. The statistical treatment based on residual and error analysis were carried to obtain significant models for Cr(VI) and Cu(II) removals. Numerically optimized coating parameters were experimentally validated and used to coat different commercially available filter matrices to select the most suitable filter platform for the coating. Based on the integrity of the coating when exposed to different water chemistries potential membrane filter materials were selected. The resulting coating was characterized and further tested for Cr(VI) and Cu(II) removals. The potential uptake mechanisms of the coating was also investigated.

2. EXPERIMENTAL PROCEDURES

2.1 Materials. GO used for the coating was synthesized using the modified Hummer's method²⁷ starting from graphite (<45μm), which was purchased from Sigma Aldrich. Chitosan (low molecular weight), polyethyleneimine (50% wt/wt% in water) and, glutaraldehyde (25% w/w% in water) were also purchased from Sigma Aldrich. Whatman qualitative 2 cellulose filter papers for the optimization process were purchased from Fisher Scientific. Glass microfiber type 691 (pore size 1.5 μm), nylon (pore size 1 μm), polyethylene/polypropylene (pore size 10 μm), polytetrafluoroethylene (PTFE) type TE 36 (pore size 0.45 μm), PTFE type TE 37 (pore size 1

- μm), cellulose acetate type OE 67 (pore size 0.45 μm), and cellulose acetate type OE 68 (pore size
 μm) membrane filters were purchased from VWR international. Sodium chloride crystals (≥
 99.0% assay), sodium bicarbonate powder (99.5 100 % assay), acetic acid (≥ 99.7%) were also
 purchased from Sigma Aldrich. All the chemicals used were of analytical grade. Furthermore, all
- 5 synthetic solutions were prepared using deionized (DI) water, unless specified otherwise.

- 2.2 Characterization of GO. Synthesized GO was characterized using attenuated total reflectance infrared (ATR-IR) spectroscopy, X-ray photoelectron spectroscopy (XPS), scanning electron microscopy (SEM) and Raman spectroscopy to identify the functional groups on GO surface and confirm successful synthesis. For the ATR-IR analysis, samples were dried in a desiccator to remove moisture and analyzed with a Nicolet iS10 Mid Infrared FTIR Spectrometer (Thermo Fisher Scientific, USA) with air as background. Acquired data were further processed using Omnic 8 Software (Thermo Fisher Scientific, USA) and analyzed using Origin Pro8.5 software (OriginLab, Northampton, MA). Raman spectrum of the GO was measured using a Raman microscopy system (IHR320, Horiba) equipped with a 532 nm laser excitation source. SEM analysis was done to visualize the physical appearance of the GO layers. GO samples were attached to a carbon double tape and sputter-coated using a Desk V sputter (Denton Vacuum) to create a thin gold layer around the sample. Gold coated samples were analyzed with a FEI XL-30 FEG SEM (Philips) field emission scanning electron microscope.²⁸ Results are shown in the supporting information Figure S1 and Text S1.
- **2.3 Preparation of working solutions.** Stocks of materials were prepared for the synthesis of the CS-PEI-GO mixtures as followsing: 0.04% CS in 0.5% HCl, 25% PEI in 2.5% HCl and 2500 ppm GO in DI water. These stock solutions were used to prepare the different working mixtures as described in supporting information (SI) table S1. Synthetic heavy metal solutions

- 1 required for batch filtrations were made in DI water. First, the stock solutions of 500 ppm
- 2 concentration of Cr(VI) and Cu(II) were prepared by dissolving amounts of 708.6 mg and 969.9
- 3 mg of potassium dichromate (K₂Cr₂O₇, crystals, 99.8% assay) and cupric nitrate (Cu(NO₃)₂.3H₂O
- 4 crystals, 98% assay) respectively, in 500 mL of DI water. Working solutions of 10 ppm
- 5 concentration was prepared by diluting the stock solutions in DI water.
- **2.4 Experimental design using RSM.** Different mixture designs were developed using
- 7 Design Expert 10.0 from Stat-Ease Inc. (Minneapolis, USA). In the design process, four variables
- 8 (X_i) , namely soaking time in CS mixture (X_1) , GO composition (X_2) , PEI composition (X_3) and
- 9 GLA composition (X_4) were used as independent factors to create 25 randomized design points
- based on two response variables (Y_i) : Cr(VI) % removal (Y_I) and Cu(II) % removal (Y_2) .

Table 1: Independent, response and fixed variables used in the RSM mixture design for the optimization of CS-PEI-GO coating.

Parameter	Units	Minimum value	Maximum value	Variability
Soaking time in CS	Minutes	10	30	Discrete
CS composition	wt%	N/A	0.04	Fixed
GO composition	ppm	250	1000	Continuous
PEI composition	wt%	1	3	Continuous
GLA composition	wt%	1	3	Continuous
Soaking time in PEI-GO-GLA	Minutes	N/A	30	Fixed
% Cr(VI) removal	-	N/A	N/A	N/A
% Cu(II) removal	-	N/A	N/A	N/A

Soaking time in the CS mixture was considered as a discrete parameter with three steps; while other independent parameters were considered as continuous parameters within a selected range based on the preliminary studies. Ranges for those four components are given in Table 1.

Percentages given in the mixture design were translated into weight terms considering a 10-g batch of the working mixture. Remainder weight was completed by adding required amounts of DI water

as presented in the 6th column of table S1. All the design points were analyzed in triplicates.

2.5 Preparation of the coating. Cellulose membranes were coated by dip coating. First, they were soaked in 0.04% CS solution for the desired time as mentioned in the 2nd column of the table S1. Six or more filters were used to coat with each mixture, as experimental replicates. In the meantime, required amounts of PEI, GO, and DI water were weighed in a separate glass vial based on the respective mixture design compositions as mentioned in the table S1. The PEI-GO-water mixture in the glass vial was shaken thoroughly using a vortex for around 5-10 minutes to ensure a homogeneous solution. GLA was added to the homogenized mixture quickly and mixed for another minute using the vortex. This mixture was poured immediately into another clean petridish, and filters pre-soaked in CS were carefully transferred to a new petri-dish containing the homogeneous mixture of PEI-GO-GLA. After dip coating for a fixed time of 30 minutes, CS-PEI-GO coated filters were rinsed with DI water and air-dried. Then, the filters were wrapped in aluminum foil and were stored under dry conditions until further use. Fresh batches of filters were made ahead of each experiment to avoid unnecessary effects of aging and storage conditions.

2.6 Contaminant removal experiments. As explained earlier, 25 different filter coatings were prepared and used for the batch filtration of 20 mL aliquots of Cr(VI) and Cu(II) solutions with an initial concentration of 10 ppm. A NE-300 Just Infusion syringe pump (New Era Pump Systems. Farmingdale, NY) was used to perform filtrations with a liquid feed rate of 5 mL/min.

Filtered samples were analyzed with a flame atomic absorption spectrometer (AAS) (AAnalyst 200, Perkin Elmer). Cu(II) samples were acidified by adding a drop of concentrated nitric acid. For both Cr and Cu analyses, air was used as the oxidant with acetylene flows of 3.3 and 2.5 L/min respectively. To generate the calibration curve, standards up to 5 ppm were prepared, which were adequate to cover the linear ranges of each metal. Samples with lower removals were diluted before

6 the AAS measurements to match the linear ranges of each element. Percentage removals for each

7 filtration were calculated using eq 1.

8
$$\% Removal = \frac{Initial conc. - Final conc.}{Initial conc.} \times 100\%$$
 (1)

2.7 Statistical analysis and the optimization of the coating. Percentage removals obtained from the contaminant removal experiments were used for the statistical analysis using the Design Expert software version 11 (Stat-Ease, Inc., Minneapolis). Using the set of independent variables presented earlier, a mathematical expression in the form of a quadratic equation (eq 2) was developed to fit the obtained data.

14
$$Yi = \beta_0 + \sum_{i=1}^n \beta_i x_i + \sum_{i=1}^{n-1} \sum_{j=i+1}^n \beta_{ij} x_i x_j + \sum_{i=1}^n \beta_{ii} x_i^2$$
 (2)

Here, β_0 is the offset coefficient, which is a constant. Other coefficients for the linear effect, interaction effect, and quadratic effect are β_i , β_{ij} , and β_{ii} , respectively. Obtained data were subjected to various statistical optimization, such as residual analysis, surface analysis and numerical optimization to find an optimized solution for the filter coating conditions. Obtained optimized solution was experimentally validated by synthesizing the suggested optimal coating with cellulose qualitative 2 filters and performing contaminant removals for Cr(VI) and Cu(II) to verify whether the expected removal and actual removal matched the accuracy of the model. Experimentally validated coatings were used to coat different filter matrices and were subjected to stability check.

2.8 Selection of a base membrane based on stability of the coating. A stability check was carried out to select a more suitable base membrane. First, dip coatings were done on different commercially available filter matrices with the optimized CS-PEI-GO coating parameters. Coated filters were characterized using ATR-IR spectroscopy to ensure the successful coating. The stability of the coated filters were checked by exposing them to various aqueous solutions at different time lengths: 1, 4 and 24 hours. The aqueous solutions used were a) water; b) saturated sodium chloride solution c) saturated sodium bicarbonate solution and d) 4.5% acetic acid solution. The water used was fresh deionized water with a near pH~7.0 to simulate freshwater. A saturated sodium chloride solution was prepared by dissolving 35 g of sodium chloride crystals ($\geq 99.0\%$ assay) in 100 mL of DI water. This solution aimed to simulate water with high salinity (brine) that could occur in the environment. Saturated sodium bicarbonate solution was prepared by dissolving 8 g of sodium bicarbonate powder (99.5 – 100 % assay) in 100mL of DI water. The resulting solution had a basic pH of ~ 8.3 to simulate freshwater with more basic pH. Finally, 4.5% acetic acid solution with pH ~ 2.4 was prepared by slowly adding 4.78 mL of 99.7% acetic acid concentrate per 100 mL of DI water. This acidic solution aimed to simulate the treatment of more acidic water samples during filtration.

1

2

3

4

5

6

7

8

9

10

11

12

13

14

15

16

17

18

19

20

21

22

23

Aliquots of 5 mL of each solution were added to each well in 6-well plates to dip the coated filters into these different solutions for 1, 4 and 24 h time intervals. Thereafter, they were removed from the solutions and dried inside a desiccator before analyzing with the ATR-IR. Three or more replicates were tested for each scenario.

2.9 Characterization of the optimized coating on the selected base membrane. Base membrane selected via the stability check was coated with the optimized CS-PEI-GO coating. They were characterized using SEM, XPS and thermogravimetric analysis (TGA). TGA of CS-

1 PEI-GO coated and uncoated membranes were carried out to investigate the thermal stability of

2 the modified filters. The analysis was carried out with samples weighing 5-7 mg, at a temperature

gradient of 10 °C per minute in O2 atmosphere. An O2 flux of 40 mL/min and N2 flux of 60

mL/min was used while the temperature was changing from 25 to 600 ° C.

Gravity-filtration was performed with CS-PEI-GO coated and uncoated membranes to investigate the effect of coating in flow rates. A clean 47-mm glass filtration set was used for the gravity filtration. This filtration set included a cylindrical filter funnel, filter head and funnel support base held together with a clamp. Each filter membrane was placed between the filter head and the bottom of the filter funnel and clamped to ensure no leaks from the glass fittings. A volume of 500 mL of DI water was passed through the filter under gravity and time taken for each filtration was measured using a stopwatch. Flow rates (L/m²s) were calculated via normalization of the filtration volume by filtration time and coated filter area available for filtering. In this case, the available coated filter area was 9.6 cm².

2.10 Batch removal of contaminants. CS-PEI-GO coated membranes characterized earlier were further analyzed to demonstrate the removal efficiency of Cr(VI) and Cu(II). Removal efficiencies were measured in both single contaminant systems and binary-contaminant systems, i.e. containing both Cr(VI) and Cu(II) ions. Synthetic heavy metal solutions containing various initial concentrations: 1, 10, and 20 ppm, were prepared by diluting the metal stock solutions with DI water. Batches of 20 mL of these solutions were filtered in triplicates and analyzed with AAS. Percentage removals were calculated using eq 1. XPS analysis was carried out to confirm the successful adsorption of Cr and Cu onto the CS-PEI-GO coated filters used for the contaminant removals in single component systems.

3. RESULTS AND DISCUSSION

an I-optimal design approach because of the flexibility in controlling the constraints. With this approach, the factors can be controlled within a continuous range or as discontinuous levels based on the nature of the parameter. For example, in this design, the soaking time in CS was a factor with 3 levels (ex: 10, 20 and 30 minutes), while factors like GO composition and PEI composition were in continuous ranges. An I-optimal algorithm was chosen since it is recommended to build response surface designs where the goal is to optimize the factor settings while having higher precision. The complete list of responses from the contaminant removal experiments is listed in table S1. Values for the removals of Cr(VI) and Cu(II) are averages of three or more replicates for each design point. These removal data were fitted into a quadratic equation as proposed by eq 2. Resulting expressions for Cr(VI) and Cu(II) removals are presented by eq 3 and eq 4 below.

$$Y_{1(\% \ Cr \ removal)} = 63 + 6.3x_1 + 9.2x_2 + 3.8x_3 + 6.7x_4 - 1.9x_1x_2 + 8.3x_1x_3 - 1.4x_1x_4 - 2.4x_2x_3 + 3.7x_2x_4 - 0.37x_3x_4 + 9.6x_1^2 - 2.6x_2^2 + 14x_3^2 + 4x_4^2$$
 (3)

$$Y_{2(\% Cu \ removal)} = 19 - 0.2x_1 + 1.3x_2 + 2.6x_3 - 3.1x_4 - 5.1x_1x_2 - 2.9x_1x_3 + 1.4x_1x_4 + 3x_2x_3 - 1.8x_2x_4 - 0.3x_3x_4 + 7.6x_1^2 - 4.1x_2^2 + 2.5x_3^2 - 4.7x_4^2$$

$$(4)$$

Higher values of the coefficients and constant terms in eq 3 proposes that higher removals can be expected from the Cr(VI) removal compared to Cu(II), which was evident even in the actual results presented in table S1.

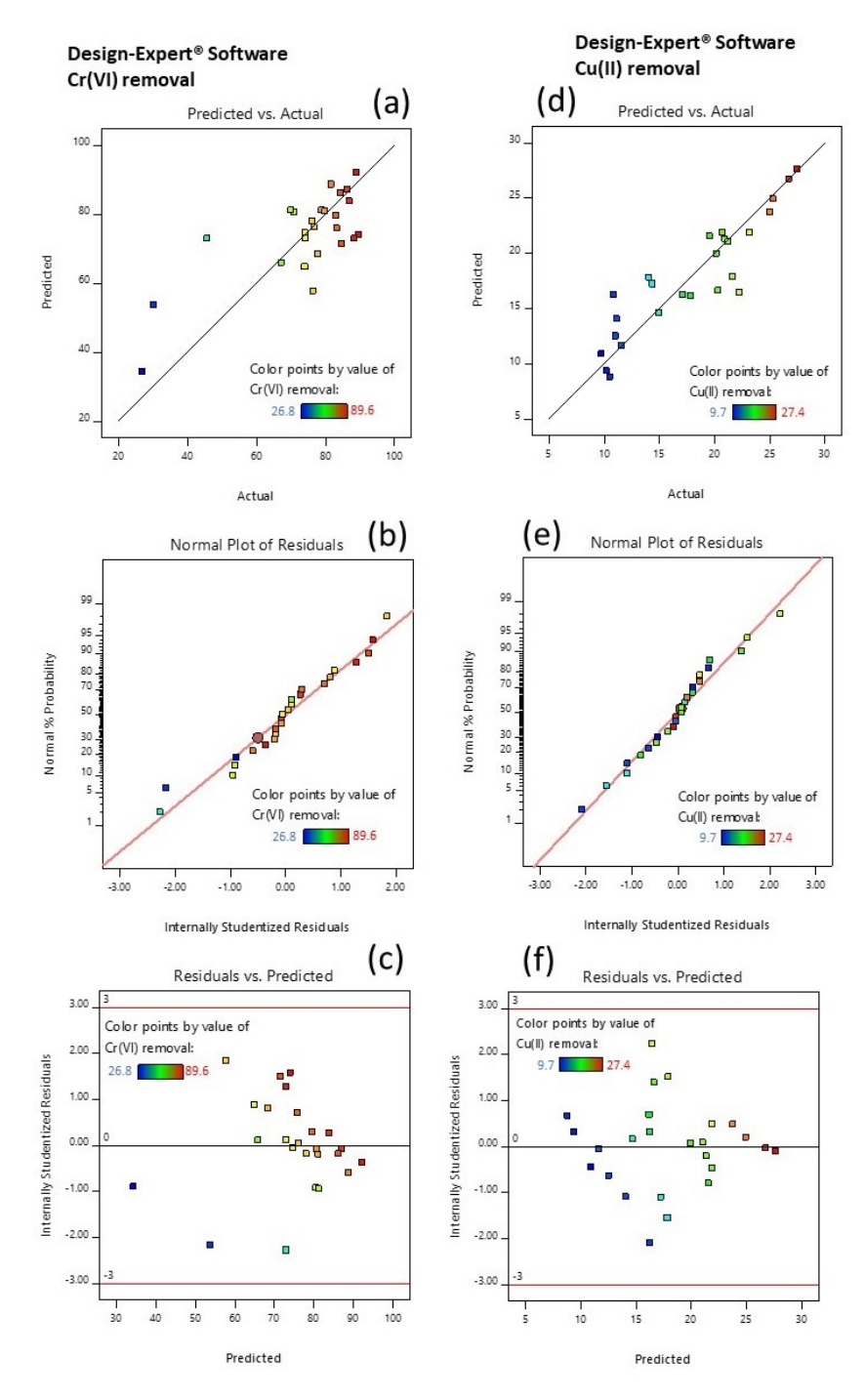


Figure 1: Residual plots for Cr(VI) and Cu(II) removal responses. Predicted vs actual responses for (a) Cr(VI) and (b) Cu(II) indicate that predicted values are in agreement with the actual results; therefore no transformation of data is needed. Normal probability plots for (c) Cr(VI) and (d) Cu(II) indicate the residuals follow a normal distribution as they follow a straight line in the normal probability plot. The diagnostics for outliers for (e) Cr(VI) and (f) Cu(II) indicated that no outliers were present outside the \pm 3 set limit.

Analysis of variance (ANOVA) was used to assess the significance of each term in the model equations. The analysis was based on the partial probability values (*p*-values) where *p*-values of less than 0.05 indicates that the terms in the model are significant. First, for the Cr(VI) removal, for the full quadratic model eonsideredobtained presented, smaller *F*-value of 1.21 and a higher *p*-value of 0.39, which indicated that the model is not significant. However, the The model for Cr(II) removal showed R² of 0.63, which is acceptable for RSM models.²⁹ R² values close to 1 indicate better predictability of the model, which agrees with the actual and predicted responses.²¹,

On the other hand, for Cu(II) removal, the F-value of 3.39 and p-value of 0.03 indicated that the model is significant. These values suggest that there is a 2.91% chance that the model F-value is due to random error. When considering the R², the coefficient of determination, which is a measure of the ability of the model in making predictions, Cu(II) model showed R² of 0.83 indicating a better predictability when compared to the model for Cr(VI) removal. In order to obtain significant models for both Cr(VI) and Cu(II) removals, non-significant terms were removed from the quadratic model using a backward calculation method. Obtained modified model equations for Cr(VI) and Cu(II) removals are given by eq 5 and eq 6 respectively.

$$Y_{1(\% \ Cr \ remov} = 75.7 + 6.1x_1 + 9.6x_2 + 1.4x_3 + 4.3x_4 - 10.9x_1x_4 - 14.4x_2x_3$$
 (5)

$$Y_{2(\% Cu remov} = 19.9 - 0.8x_1 + 1.8x_2 + 3.3x_3 - 3.3x_4 - 4.2x_1x_2 + 8.2x_1^2 - 5.7x_2^2 - 4.7x_4^2$$
(6)

After the modification, the model for Cr(VI) removal became significant with increased F-value of 3.76 and decreased p-value of 0.01, due to the removal of the non-significant terms. Cr(VI)

removal also showed better goodness of fit as the standard deviation of the model decreased from 15.6 to 12.7. Similarly, a more significant model was obtained for Cu(II) removal with a reduced quadratic model, which led to an increased *F*-value of 9.03 and decreased *p*-value of 0.0001. In addtion, the standard deviation of the model decreased from 3.7 to 3.0 showing the improved goodness of fit of the model. Furthermore, the adequate precision values, which is a measure of the signal to noise ratio of RSM models, were obtained for the models to compare the predicated removals and pure error of the predicted error. Values of 8.6 and 10.6 were obtained for Cr(VI) removal and Cu(II) removal respectively, since a value higher than 4 is typically desired, these results indicate adequate signal.^{21,30}

Residual diagnostics were used to further evaluate the obtained modified models. Here, the residuals are defined as the difference between the actual responses and the responses predicted by the model. As shown in Figure 1b, residuals for both responses (Cr(VI) and Cu(II) removals) closely followed a straight line through the origin in the normal probability plot. These results indicate that the residuals of the obtained data followed normal distributions. As a result of this phenomenon, no transformations were required to predict the results. Figure 1c illustrates that the residuals for both responses were distributed within a very narrow range. This observation indicates that there were no outliers present, compared to the set limit of \pm 3. In conclusion, the diagnostic analysis indicated that the obtained models were suitable for predicting Cr(VI) and Cu(II) removals.

Additional analysis of the model parameters was done using the surface plots. RSM allows to look at the individual and combined effects of independent variables on the response variables with the aid of these surface plots. This analysis allows to maintain certain factors at a fixed level and study the influence of other factors using the surface plots according to the obtained data.

- 1 Figures 2 and 3 provide graphical representations of various surface plots for combinations of two
- 2 independent variables for Cr(VI) and Cu(II) removals, respectively.

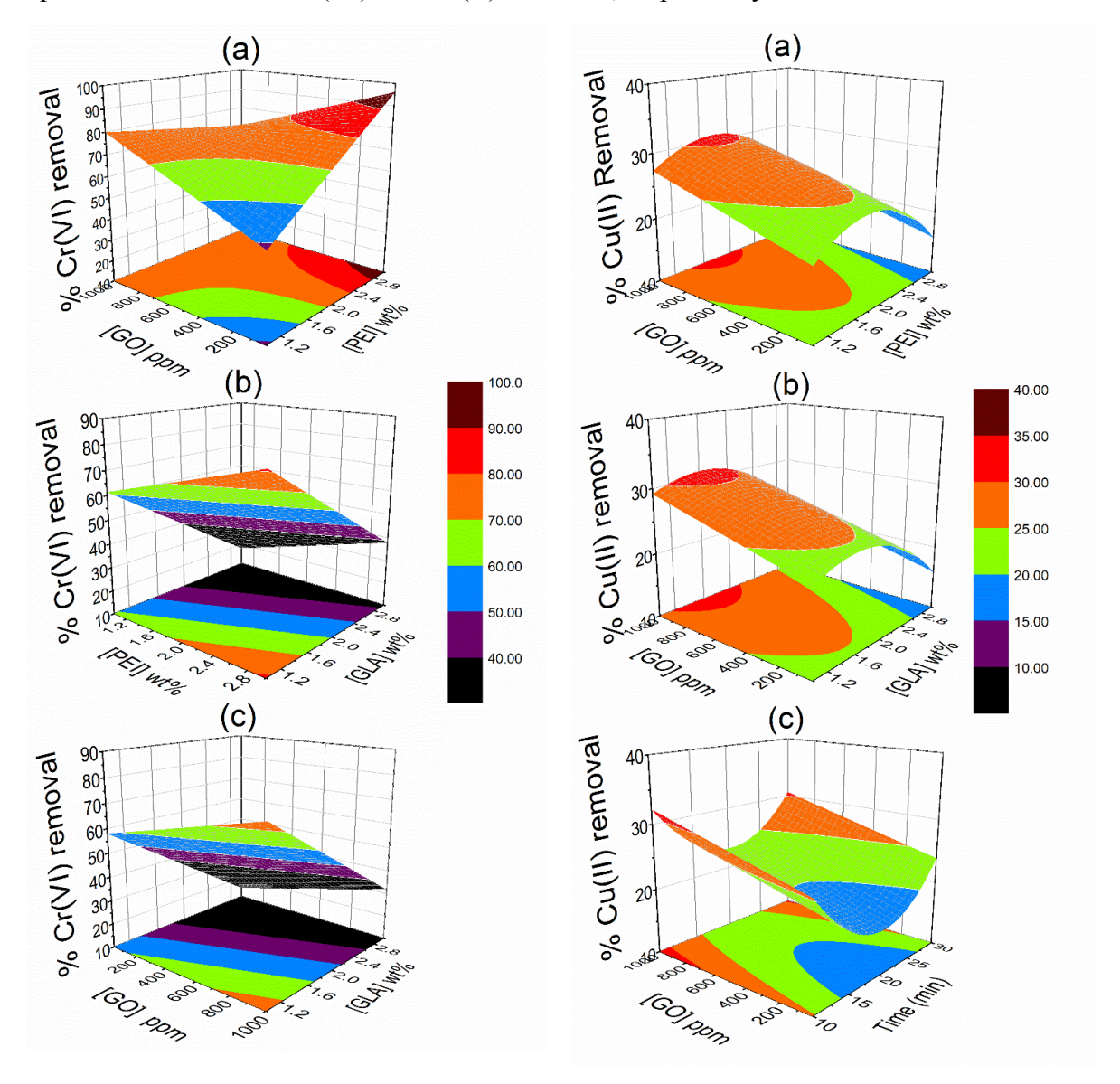


Figure 2: Surface plots for Cr(VI) (a) GO concertation, [GO] vs [PEI] shows increasing concentrations of GO and PEI lead to increasing Cr(VI) removal (b) [PEI] vs [GLA] and (c) [GLA] vs [GO] also show highest higher removals achieved when both factors are at the highest of their respective ranges. For all these plots, other independent variables were fixed at the middle of their range.

Figure 3: Surface plots for Cu(II) (a) [GO] vs [PEI] and (b) [GO] vs [GLA] at 30 minutes of soaking time show that highest higher removals were achieved when [GO] is at its highest of the range and the other factors considered were in the mid-range and; (c) time soaked in CS vs [GO] shows much higher removals when [GO] and time are the highest of their respective ranges.

In the surface plots presented in Figures 2 and 3, the fixed levels for the independent variables were set at the middle level of their selected ranges to simplify interpretation. As Figure 2a illustrates, when the GO and PEI concentrations increased, the Cr(VI) removal also increased. In previous studies, it has been shown that the inclusion of PEI provides extra amine groups in the nanocomposite, which are capable of protonation when exposed to acidic conditions. This protonation results increase in electrostatic attraction of negatively charged ions, such as the Cr(VI) in the form of Cr₂O₇²⁻, in this case. Slightly acidic conditions provided by the dissociation of K₂Cr₂O₇ help this phenomenon during filtration, therefore, increasing the percentage removal of Cr(VI). On the other hand, GO plays a significant role in removing Cr species through its oxygen containing groups on the surface. In Figures 2b and 2c, the increase in Cr(VI) removal corresponds to the increasing in PEI and decreasing in GLA concentrations. In the synthesis of the nanocomposite coating, GLA serves as a crosslinking agent and, hence, consumes amine groups while producing imine groups. Imine groups are still capable of protonation and can produce electrostatic attraction of negatively charged Cr(VI) ions to allow its removal.

In addition to PEI, GO, and GLA effects over Cr(VI) removal, the soaking time in CS always showed an upward curvature, upholding a positive effect on Cr(VI) removal (Figures S2a and Figure S2b). The soaking time can be considered as a measure of the thickness of the CS layer. In other words, higher soaking time means a larger CS layer and more availability of amine groups. The thicker CS layer will have more amine groups than thinner layers since the crosslinking reactions consume some of these amine groups and make them unavailable for Cr(VI) removal. This issue of less availability of amine groups from CS due to the GLA crosslinking was addressed in this study by incorporating a second polymeric material, PEI, which is rich with primary and secondary amines. In addition, the slightly acidic condition generated by the chromium solution

provides protonation of PEI allowing uptake of anionic metal ions via electrostatic attractions.
 33

In the case of copper, as shown in Figure S3a and Figure 3, the inclusion of more CS by increasing the soaking time provided more favorable conditions for its removal. A thicker CS layer increased the availability of amine functional groups for Cu(II) ions to form a shared bond or a surface complex with a pair of electrons from the nitrogen atoms in the amine groups. However, the GLA concentration played a negative role in Cu(II) removal, as seen by the surface plots of GO and GLA concentrations (Figure S3b) and PEI and GLA concentrations (Figure S3c). The increase in soaking time to 30 minutes led to increasing removal of copper, as shown in Figure 3b, confirming the earlier findings that not only the amount of CS but also the consumption of amines from CS by GLA during the crosslinking process will affect Cu(II) removal. In the increase in S0 and S1 and S1

As a summary of the surface plots, Cr(VI) removal is favorable when the GO, PEI, GLA concentrations and soaking time in CS are at their highest ranges. Cu(II) removal is also favorable when the GO concentration and soaking time in CS is at their highest. But the removal of Cu(II) is more favorable with a medium range of PEI and GLA concentrations, therefore we can expect a combination of these observations from the optimized solution composition of the coating.

3.2 Optimization of the coating components and experimental validation. An optimized solution for the soaking time in CS and combination compositions of GO, PEI and GLA were selected to accommodate the removal of both contaminants. A desirability function was defined for response as given by the following equation.

$$d_{i}(\text{desirability}) = \frac{(\text{calulated } y_{i} - \text{minimum } y_{i})}{(\text{maximum } y_{i} - \text{minimum } y_{i})}$$
(7)

- 1 Geometric mean of the individual d_i values calculated for the two responses were used as the
- 2 objective function of the optimization. To find an optimum solution with more emphasis on Cu(II)
- 3 removals, as Cu(II) removals were lower, a weight of 10 was given to the desirability function of
- 4 Cu(II) removal. Therefore, the final objective function can be given by the following equation.

$$D = (d_{Cr}.d_{Cu}^{10})^{1/2}$$
 (8)

6

7

8

9

10

11

As the goal for the To achieve numerical optimization, the soaking time in CS was fixed at 30 minutes (highest possible value in the selected range) to ensure more CS in the nanocomposite in order to aid Cu(II) removal. All the independent variables mentioned were kept in the range specified earlier and both responses were subjected to maximization. The solution with the highest desirability function was chosen to be validated experimentally. The optimization determined that the optimum soaking time in CS was 30 minutes and GO concentration was 1000 ppm, both values

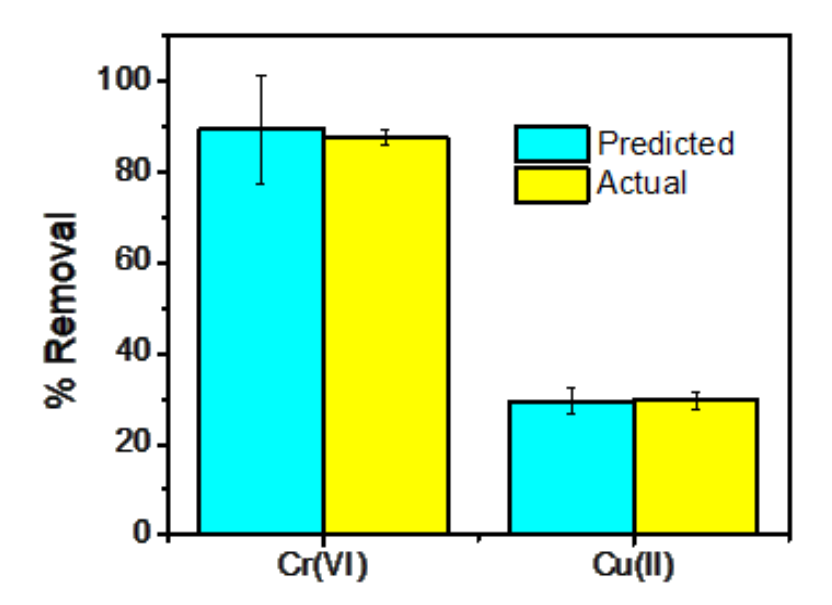


Figure 4: Predicted and actual removals for Cr(VI) and Cu(II) at 10 ppm with the optimized CS-PEI-GO coated cellulose membranes indicates that the predicted and actual removals are not statistically different. Error bars correspond to the standard deviation.

are the highest of the selected range for each factor. For PEI and GLA, the optimum concentrations were 1.95% and 1.68%, respectively.

The predicted removal of Cr(VI) and Cu(II) were 90±10 % and 30±3%, respectively, with a desirability of 0.99. This combination was tested in the lab to validate the optimization. Figure 4 summarizes the results. The results showed no statistical difference of the predicted removals and actual removals. This allowed us to conclude that the experimental validation of the CS-PEI-GO coating was aggregableagreed with the predictions. These optimized conditions were used for the selection of the best filter material for coating.

3.3 Selection of the base membrane presenting the most stable coating with the optimized mixture. The optimized composition for CS-PEI-GO coating was used to dip coat a list of commercially available filter matrices described in the materials and methods. Successful fabrication of the dip-coated filters was determined initially by visually inspecting uniformity of the coating and changes in the physical aspects of the filters. Using these criteria, some of the filter matrices were ruled out from proceeding to the next step, as they were unstable or heavily-deformed after the dip coating and drying process.

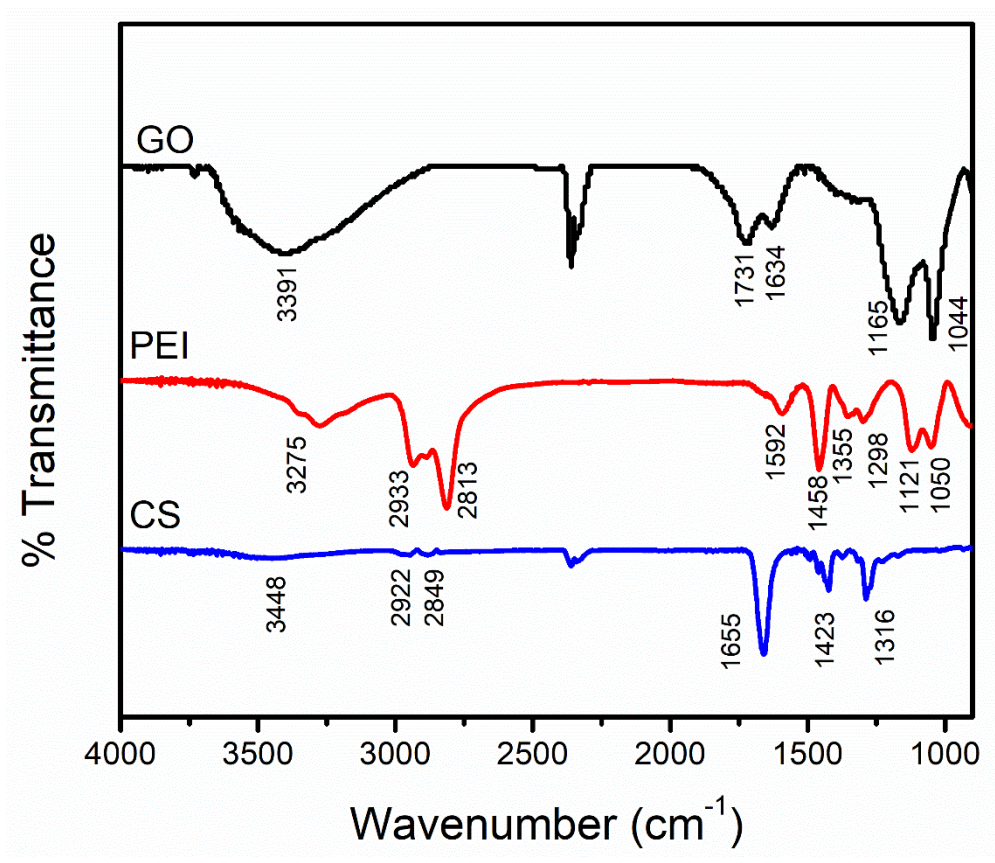


Figure 5: ATR-IR spectra of GO, PEI and CS show the characteristic peaks for each of the materials. From these peaks, most significant peaks; the broad peaks around 3100-3500 cm⁻¹, which are attributed to OH (from GO and CS) and NH₂⁻ (from CS and PEI), and 2750-3000 cm⁻¹, which are attributed to CH vibrations from CH₂ and CH₃ (from CS and PEI), and the peak at 1650 cm⁻¹, which is assigned to carbonyl stretch of –NHCO– group were considered when deciding the stability of the coating.

The ATR-IR spectrum of the GO, CS and PEI are shown in Figure 5. Identifying individual spectrum is important when investigating the integrity of the coating later in the process. In the spectrum for PEI, dominant peaks can be seen at 1050, 1121, 1298, 1355, 1458, 1592, 2813, 2877, 2933 and 3275 cm⁻¹. The peak at 1050 cm⁻¹ is assigned to C-N bonds³⁴, while the peak at 1121 cm⁻¹ is assigned to stretching of C-O bond.³⁴ The peaks at 1298 and 1355 cm⁻¹ can be attributed to C-N stretching, while the peak at 1458 cm⁻¹ can be assigned to the C-H bending.³⁵ The peak at 1592 cm⁻¹ corresponds to the N-H bending.^{21, 35} The peak at 2813 and 2933 cm⁻¹ are attributed to the

stretching vibrations of CH₂ and CH₃ respectively.³⁴⁻³⁵ Finally, the peak at 3275 cm⁻¹ can be assigned to the N-H bond.³⁴⁻³⁵

The ATR-IR spectrum of CS has dominant peaks at 1316, 1423, 1655, 2849, 2922, and 3448 cm⁻¹ wavelengths. The peak at 1316 cm⁻¹ can be assigned to CH₂; while 1423 cm⁻¹ is assigned to the signal coming from primary amine groups. The peak at 1655 cm⁻¹ can be assigned to the carbonyl stretch of –NHCO– group. Two peaks appear at 2849 and 2922 cm⁻¹, which can be attributed to the stretching vibrations from CH₂ and CH₃, respectively. The broad peak in the range of 3000 – 3500 cm⁻¹ can be attributed to the signals from -OH and -NH₂. The broad peak in the

For each coated filter type exposed to different solutions, the integrity of the coating was investigated based on the multiple peaks that appeared in their ATR-IR spectra. For the CS-PEI-GO coated filters, the broad peaks around 3100-3500 cm⁻¹, which is attributed to OH (from GO and CS) and NH₂-(from CS and PEI), and the peaks around 2750-3000 cm⁻¹, which is attributed to CH vibrations form CH₂ and CH₃ (from CS and PEI), and the peak at 1650 cm⁻¹, which is carbonyl stretch of –NHCO– group or the carbonyl results from the crosslinking were considered as the basis for deciding stability of the coatings.

For CS-PEI-GO coated cellulose Q2 filters, all the mentioned peaks were visible for all the conditions studied. A reduced intensity was observed for the CH peak at around 2750-3000 cm⁻¹ region when exposed to the brine solution for 24 hours, but the availability of other peaks confirms the stability of the coating. For the CS-PEI-GO coated GMF membranes, the OH and NH₂⁻ peaks were very broad but still visible in all the conditions studied as shown in the Figure 6. When exposed for 24 hours to NaHCO₃, the peak attributed to carbonyl bond was recorded with reduced intensity, but still considered as a stable coating. Similarly, PTFE membranes coated with the optimized CS-PEI-GO coating showed a stable coat for all the conditions, however, showed a

broad peak for OH and NH₂⁻. Finally, the CS-PEI-GO coated cellulose acetate filters also showed stability when exposed to all the studied solutions. Peaks for CH bonds and OH were very broad and had reduced intensity; however, the unchanged carbonyl peak suggested the integrity of the coating for the longest exposure time investigated. Based on these observations from ATR-IR spectra summarized in Figure 6, GMF was chosen to be the filter matrix that showed more integrity than the other materials tested.

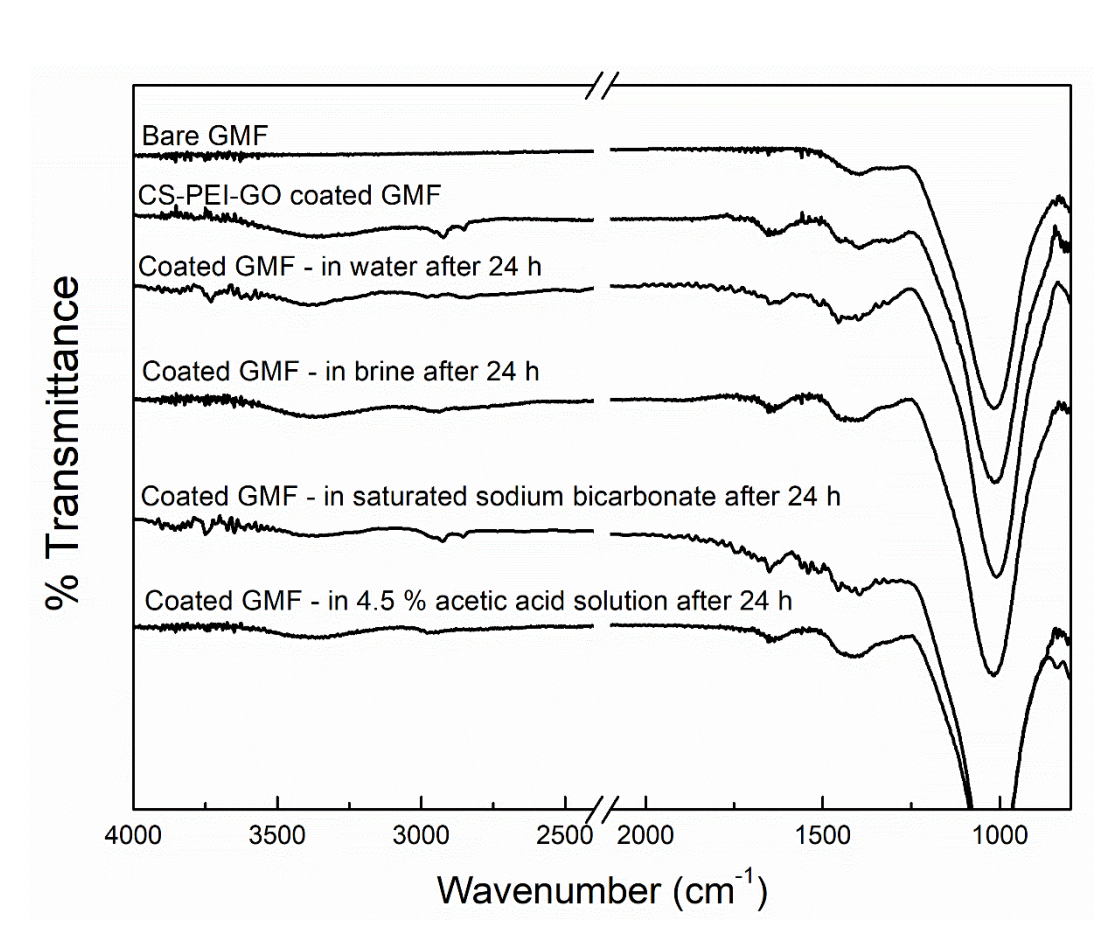


Figure 6: Spectra corresponding to the ATR-IR analysis of CS-PEI-GO coated GMF filters that were exposed for 24 hours to different test reagents solutions: water (pH~7), NaCl (pH~7), NaHCO₃ (pH~8.3) and 5% CH₃COOH (pH~2.4).

In addition to these observations, to further validate the selection of GMF as the base filter material for the later investigations, CS-PEI-GO coated GMF filters were used to remove Cr(VI) and Cu(II) at 10 ppm initial concentrations. Though both cellulose and GMF were resistant to

treatments, as indicated by the smaller removals, GMF showed much better removals of the contaminants than cellulose when <u>ethey were coated membranes</u> with CS-PEI-GO, as shown in the figure S5 in supporting information. Therefore, GMF was selected as the best filter matrix for CS-PEI-GO coating and this filter matrix combination was <u>further</u> characterized and <u>further</u> studied.

3.4. Characterization of the optimized CS-PEI-GO coating. Freshly synthesized CS-PEI-GO coated GMF filters were characterized using SEM, XPS, FTIR, and TGA. Figure 7 shows the (a) bare GMF membrane and (b) the microstructure of the CS-PEI-GO coated GMF membranes. The SEM images demonstrated successful coating of the membrane. To further confirm the coating and determine whether there were any changes of flow rates due to coating, we performed gravity filtration. The flow rate increased from 227 Lm⁻¹s⁻¹ to 411 Lm⁻¹s⁻¹ after the CS-PEI-GO coating. This increasing flow rate compared to the bare membrane can be explained by the incorporation of CS on the surface and membrane pores. CS is a hydrophilic compound and therefore facilitated the flow of the water through the pores. For the obtained results, two-tailed t-tests with α=0.05 were done to quantify the statistical significance. For CS-PEI-GO coated GMF

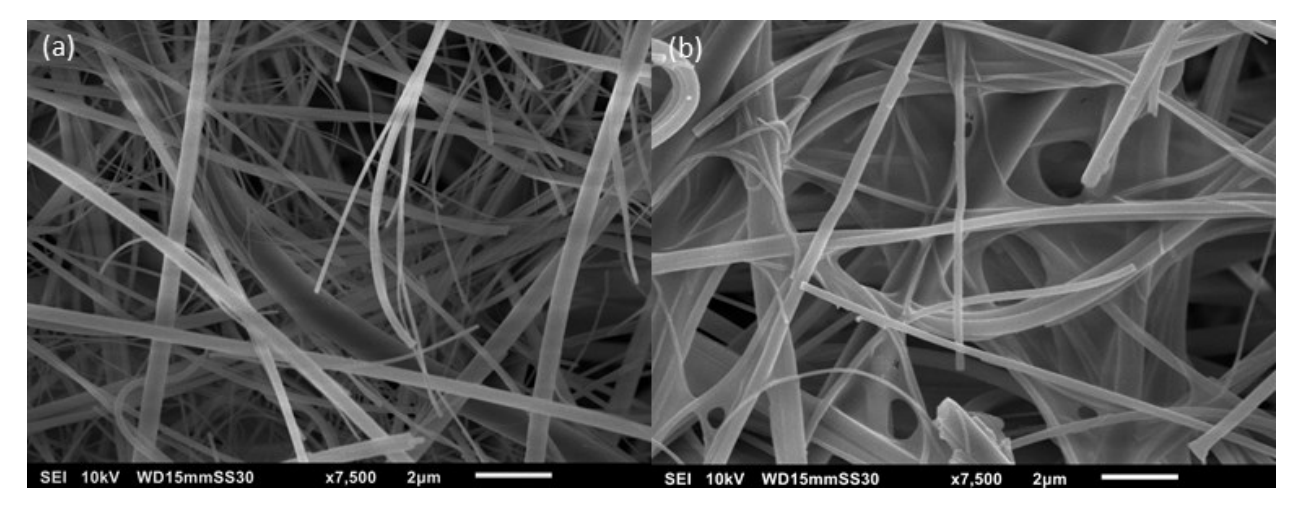


Figure 7: SEM images of (a) uncoated GMF membrane and (b) CS-PEI-GO coated GMF membranes.

membranes, an obtained *P*-value of 0.0003 suggested that the increment of the flow rate is statistically significant compared to the flow rate with uncoated GMF membranes.

Earlier, ATR-IR was used to identify the functional groups of the CS-PEI-GO on the coated membrane (Figure 4). Availability of functional groups was further evaluated by using XPS analysis. The obtained spectrum is shown in Figure 8. The wide scan of the bare GMF membrane showed peaks of Si 2s, C1s, and O1s at the binding energies of 154, 285 and 534 eV. Wide scan XPS spectrum of the coated CS-PEI-GO on GMF membranes showed major peaks at binding energies of 155, 287, 397 and 533 eV, which are attributed to Si 2s, C 1s, N 1s, and O 1s.^{21, 36}

Based on the atomic percentages, C/O and Si/O ratios of the bare GMF membrane were calculated as 7.5 and 0.34. There was no significant peak attributed to N in the wide scan of the

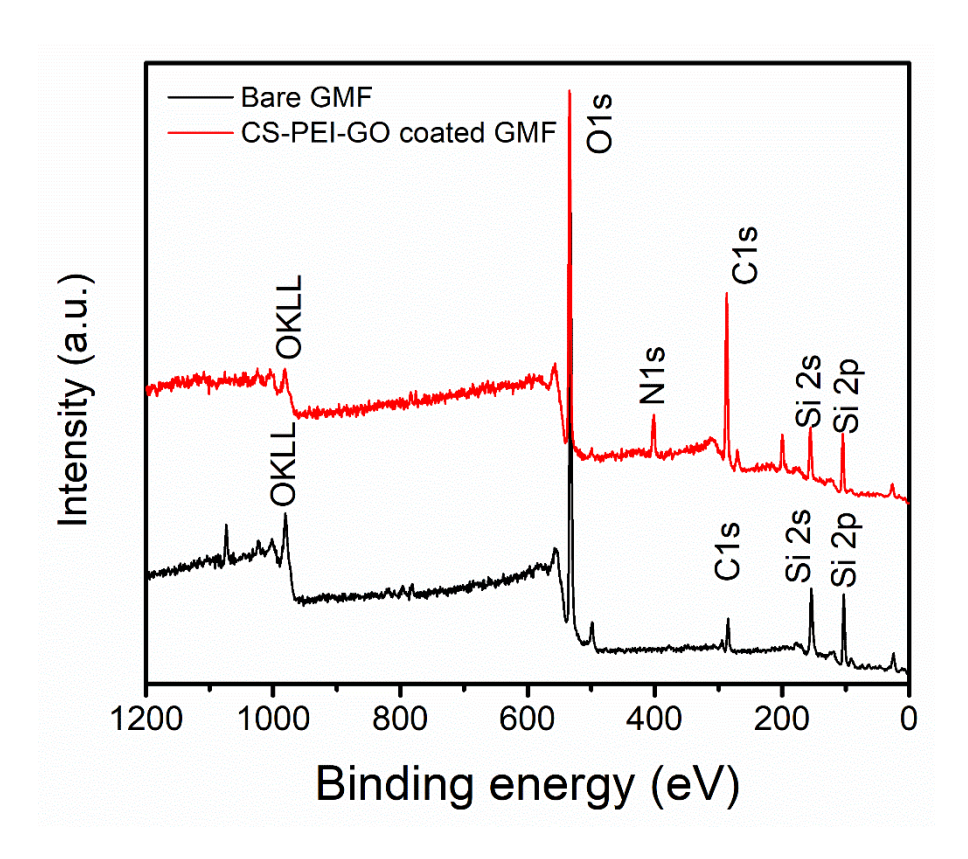


Figure 8: XPS wide scans of bare GMF membrane and CS-PEI-GO coated GMF membrane.

bare membrane. However, following the coating with CS-PEI-GO, the C/O ratio decreased to 1.1 indicating the introduction of carbonaceous groups on to the GMF filter surface. Similarly, the Si/O ratio decreased to 0.32. The increment of C and O elements on the GMF membranes was the result of the incorporation of CS and GO, as they contain multiple functional groups containing with oxygen, such as alcoholic, carboxylic and carbonyl groups. Furthermore, the wide scan of the coated GMF showed prominent N 1s peak, indicating the successful inclusion of CS and PEI, which are rich with primary amine groups.

Figure S6 illustrates TGA results obtained for CS-PEI-GO coated GMF filters. The curve for the dip coated filters presented a mass loss of ~3% when heated up to 100 °C due to water and moisture loss. GO shows a sudden mass loss from 150 to 320 °C, which can be attributed to the decomposition of its labile- oxygen- containing functional groups. The mass loss in this region was around ~30% for pure GO, however only ~13% for the CS-PEI-GO coating. Based on the thermogravimetric analysis data, grafting efficiency of the CS-PEI and CS-PEI-GO were calculated to be 25% and 27% respectively. The sum of the content of the CS-PEI and CS-PEI-GO were

Heating over 500 0 C can result in decomposition of PEI molecules. The ~7% mass loss in 500-600 0 C region has been attributed to loss of PEI in TGA analyses in previous studies. However, for the CS-PEI-GO coating, the mass loss at 500-600 0 C happened gradually and slightly at a much lower rate, indicating enhanced thermal stability of the coating compared to the raw materials. It is important to note that the coating was stable below 150 0 C, implying that the coated filters can be used in a vast range of process—temperatures. From these wide range of characterizations, it can be seen that the optimized coating on GMF membrane is stable and capable to be applied in filtering operations. The availability of multiple functional groups was confirmed indicating the ability of the coating to remove heavy metal contaminants effectively.

3.5 Heavy metal removal efficiency of the optimized coated membranes. Heavy metal removals were carried out with the CS-PEI-GO coated GMF membranes to determine the removal efficiencies. Batch experiments were earried performed out in with single and binary metal systems. For the single metal systems, three concentrations were used: 1, 10 and 20 ppm. The values were selected based on the detection limits of the AAS instrument and the acceptable levels of Cr and Cu contaminants in drinking water. Environmental Protection Agency (EPA) has provided maximum contaminant level (MCL) in their national primary drinking water regulations. MCL values for contaminants are enforceable standards for drinking water quality. MCL value for Cr(VI) is given as total chromium, set at 0.1 ppm. For Cu(II), a treatment technique has been defined instead of a MCL, set at 1.3 ppm. This regulation for copper demands to have less than 10% of the tap water samples collected to have Cu concentrations less than the action level of 1.3 ppm, within a period of one month. These MCL values are based on the nonforcible maximum contaminant level goal (MCLG), which are the levels of a contaminant in treated drinking water, at which no known or expected health effects can be observed on users. The detection limits for Cr and Cu for AAS is 0.003 and 0.0015 ppm, which is well below the acceptable limits mentioned earlier.

1

2

3

4

5

6

7

8

9

10

11

12

13

14

15

16

17

18

19

20

21

22

23

Figure 9 illustrates the data obtained for the removal of Cr(VI) and Cu(II) in single and binary synthetic solutions. In summary, CS-PEI-GO removed over 90% of both Cr(VI) and Cu(II) 1ppm initial concentration, reaching acceptable limits. Cr(VI) removals were more than 95% in average even at 20 ppm initial concentration with the GMF filters coated with CS-PEI-GO. The Cr(VI) concentration in the filtrate reached the MCL level of Cr(VI), which is 0.1ppm. Increasing initial Cr(VI) concentrations resulted in a drop of the average percentage removal, which were similar in pattern to the Cu(II) removals. There was no statistical significance shown between the

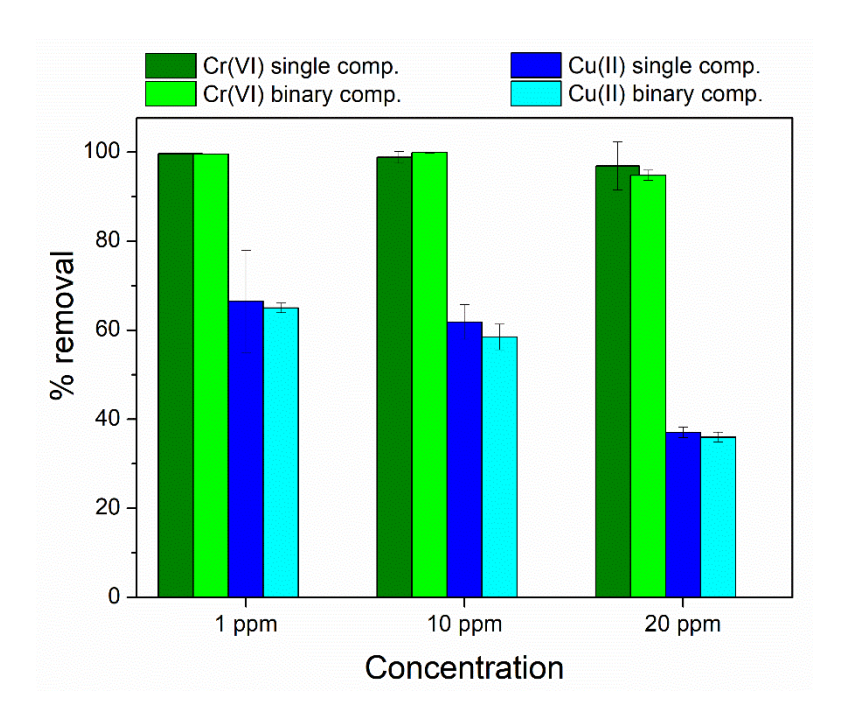


Figure 9: Cr(VI) and Cu(II) removal in single and binary component synthetic solutions of 1, 10 and 20 ppm. Cr(VI) removals were more than 95% in average even at 20 ppm initial concentration; while Cu(II) removal dropped from ~60% to <40% with increasing initial concentration. However there were no significant differences between the single and binary mixtures indicating enough adsorption sites to uptake both Cr(VI) and Cu(II) at the same time.

- 1 removals in single and binary mixtures. This indicates the availability of enough adsorption sites
 - and functional groups to simultaneously remove both positively and negatively charged metal ion
- 3 contaminants.

It is important to note that the removals for Cr(VI) and Cu(II) at 10 ppm with CS-PEI-GO coated GMF (shown in figure 4) were higher than the removals recorded for the coated cellulose quantitative 2 membranes, indicating the selection of base membrane can enhance the removal efficiencies. It is worth to note that, neither bare cellulose nor GMF membranes alone were capable of removing contaminants. GMF has a smaller and complicated pore network with pore size of 1.5 µm compared to the 8 µm pore size of the cellulose matrix. This pore size provided a coating of a larger surface area, hence having a more torturous path available for the water to go through, which allowed much better removals.

3.7 Heavy metal removal mechanisms. XPS analysis of the used CS-PEI-GO coated filters provided insights about the successful metal adsorption onto the coating and possible removal mechanisms of Cr(VI) and Cu(II). Coated GMF filters used for the filtration of single component synthetic contaminants were dried and tested for surface properties.

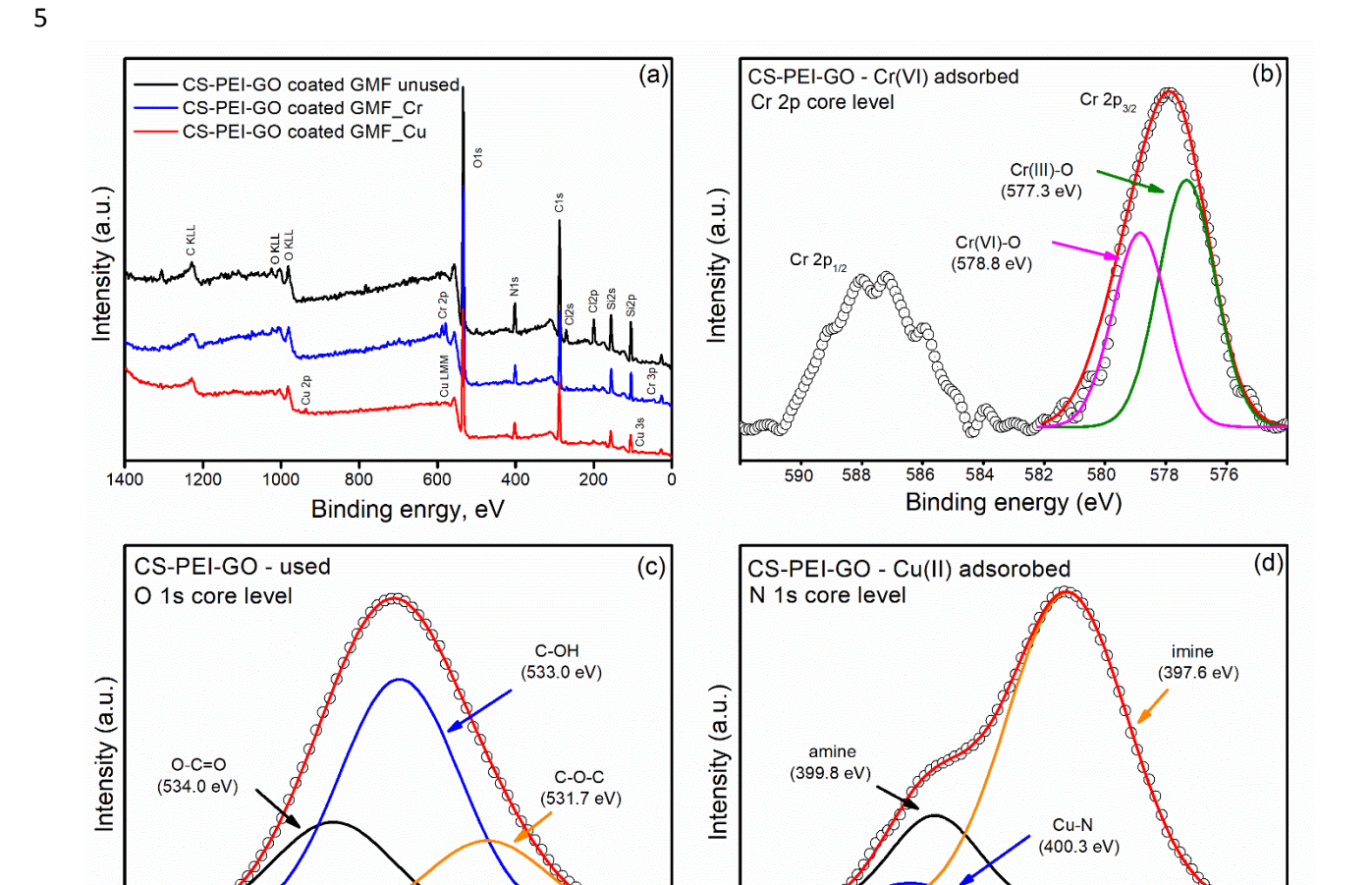


Figure 10: XPS spectra of spent CS-PEI-GO coated GMF filters. (a) Wide scans indicating signals of Cr and Cu adsorption onto the coating; (b) deconvolution of Cr 2p shows presence of Cr(VI) and Cr(III) oxidation forms on the spent filters; (c) deconvolution of O1s after Cr(VI) adsorption illustrates oxidation of graphitic carbon causing the reduction of Cr(VI) to Cr(III); and (d) deconvolution of N1s after Cu(II) adsorption shows the appearance of the new Cu-N bond.

Binding energy (eV)

Binding energy (eV)

The comparison of XPS spectra of CS-PEI-GO coated GMF filters before and after Cr(VI) adsorption given in Figure 10a showed the appearance of a new peak with a binding energy of 577.6 eV, which can be attributed to Cr 2p. Deconvolution of the Cr 2p peak showed the presence of four major peaks as shown in Figure 10b. Peaks at 577.4 and 586.9 eV can be attributed to Cr(VI) 2p_{3/2} and 2p_{1/2}, respectively. Other two peaks at 579.9 and 588.9 eV can be attributed to Cr(III) 2p_{3/2} and 2p_{1/2}, respectively.³⁹ Co-presence of Cr(VI) and Cr(III) ions analyzed with XPS showed the reduction of Cr(VI) to a less-toxic form of chromium during the adsorption process.

When considering the O1s spectrum after the Cr(VI) adsorption given in Figure 10c, it deconvolutes into three major peaks. Apart from the peaks attributed to C-O-C at 530.01 eV and C-O or OH at 531.21 eV, a new peak appeared at 532.40 eV, which can be attributed to C=O. The C=O bonds can be generated due to the oxidation of C-H and C-OH bonds suggesting a possible removal mechanism for Cr(VI) ions from the solution.^{36, 39} When Cr(VI) anions were trapped in the porous structure of the filter matrix modified with the CS-PEI-GO coating, first they are bound to the positively charged surface of CS-PEI-GO via electrostatic attraction. This is followed by the oxidation of graphitic carbons, which results in the reduction of Cr(VI) to Cr(III) completing the red-ox reaction as shown in the XPS results.^{21, 39}

Similarly, XPS analysis of CS-PEI-GO coated GMF filters used for Cu(II) filtration indicated the presence of Cu ions on the coating surface as new peaks for Cu appeared at 936, 557 and 105 eV as shown in Figure 10a. Deconvolution of the N1s peak (Figure 10d) showed three peaks, including a new peak appearing at 400.33 eV apart from the peak attributed to amine (399.80 eV) and the peak attributed to imine (397.62 eV).^{21,36}The new peak can be attributed to Cu-N bond suggesting the formation of a surface complex of Cu ions and amine. One possible mechanism is the donation of a pair of electrons from nitrogen atoms in the amine group to Cu(II),

- which formed a shared bond between copper and nitrogen. In summary, XPS provided a good
- 2 insight on successful adsorption of both Cr(VI) and Cu(II) onto CS-PEI-GO surface, while
- 3 providing solid evidence for uptake mechanisms.

4. CONCLUSIONS

4

5

6

7

8

9

10

11

12

13

14

15

16

17

18

19

20

21

22

A multifunctional nanocomposite containing CS-PEI-GO, capable of removing both negatively and positively charged metal contaminants, was successfully synthesized and optimized using RSM. Coating parameters, such as soaking time in CS, compositions of PEI, GO and GLA (for crosslinking) were optimized using RSM based on the maximum removal of Cr(VI) and Cu(II) ions. Reduced quadratic polynomial models developed for the response variable showed a good correlation between actual and predicted responses during the statistical analysis. Response surface analyses indicated the importance of higher CS soaking time and higher GO concentrations to make more amine and oxygen-containing functional groups available for the removal of the selected metals. ATR-IR based stability check and removal efficiency was employed to select a suitable commercially available filter matrix based on the integrity of the CS-PEI-GO coating when exposed to various water chemistries. Thus, GMF was selected as the most suitable filter matrix for the coating. XPS confirmed the successful adsorption of contaminants onto CS-PEI-GO coating surface. High resolution scan for Cr peaks indicated that was Cr(VI) was removed from the solution via electrostatic attraction and via redox reactions, causing oxidation of organic functional groups, while reducing Cr(VI) to the less toxic form of chromium, i.e. Cr(III). Cu(II) ions formed a surface complex with amine groups by sharing a vacant electron pair. Ability to remove both positively and negatively charged contaminants, opens up the potential for using the optimized CS-PEI-GO coating to remove other contaminants such as nitrate, microorganisms, and

- 1 other toxic various heavy metals, paving the way to further studies and to a development of a
- 2 technology that is applicable in real-world application.

3 ASSOCIATED CONTENT

4 Supporting information

- 5 Table S1 (design of experiments for RSM), Figure S1 (characterization of GO), Text S1
- 6 (characterization of GO) Figure S2 (additional surface plots for Cr(VI) removal), Figure S3
- 7 (additional surface plots for Cu(II) removal), Figure S4 (digital photos of CS-PEI-GO coated filter
- 8 membranes), Figure S5 (Cr(VI) and Cu(II) removals with CS-PEI-GO coated cellulose filters and
- 9 GMF filters), Figure S6 (TGA analysis of uncoated GMF membrane and CS-PEI-GO coated GMF
- 10 membranes)

11 AUTHOR INFORMATION

12 Corresponding author

- *Phone: +1 713-743-1495. E-mail: dfrigirodrigues@uh.edu
- 14 ORCID
- 15 Pasan C. Bandara: 0000-0001-7562-4377
- 16 Enrico T. Nadres: 0000-0002-7591-5868
- 17 Debora F. Rodrigues: 0000-0002-3124-1443
- 18 Notes
- 19 The authors declare no competing financial interest.

ACKNOWLEDGEMENTS

- 2 This work was supported by the following funds: US Department of Interior, Bureau of
- 3 Reclamation through the Desalination and Water Purification Research and Development Program
- 4 (Agreement No. R16AC00123); NPRP grant number: 9- 318- 1- 064 from the Qatar National
- 5 Research Fund (a member of Qatar Foundation); CBET NSF Career grant number: 1150255; and
- 6 NSF BEINM Grant Number: 1705511. The findings achieved herein are solely the responsibility
- 7 of the authors. Authors also would like to extend their acknowledgements to Dr. Charisma Lattao,
- 8 Dr. Hang N. Nguyen, Dr. Alison McDermott, Dr. Jem Perez, undergraduates Brittany Tinh, Alex
- 9 Morales, Olivia Kuligowski, and Rini Maiti for their contributions in the various states of the
- 10 study.

11

1

12 References

- 13 (1) Rodriguez, C.; Van Buynder, P.; Lugg, R.; Blair, P.; Devine, B.; Cook, A.; Weinstein, P.
- 14 Indirect Potable Reuse: A Sustainable Water Supply Alternative. *International journal of*
- environmental research and public health **2009**, 6 (3), 1174-1209, DOI: 10.3390/ijerph6031174.
- 16 (2) Rodriguez, C.; Weinstein, P.; Cook, A.; Devine, B.; Van Buynder, P. A Proposed Approach
- 17 for the Assessment of Chemicals in Indirect Potable Reuse Schemes. *Journal of Toxicology and*
- 18 Environmental Health, Part A **2007**, 70 (19), 1654-1663, DOI: 10.1080/15287390701434828.
- 19 (3) Bixio, D.; De heyder, B.; Cikurel, H.; Muston, M.; Miska, V.; Joksimovic, D.; Schäfer, A. I.;
- 20 Ravazzini, A.; Aharoni, A.; Savic, D.; Thoeye, C. Municipal Wastewater Reclamation: Where Do
- 21 We Stand? An Overview of Treatment Technology and Management Practice. Water Science &
- 22 *Technology* **2005**, *5* (1), 77-85.

- 1 (4) Canet, L.; Ilpide, M.; Seta, P. Efficient Facilitated Transport of Lead, Cadmium, Zinc, and
- 2 Silver across a Flat-Sheet-Supported Liquid Membrane Mediated by Lasalocid A. Separation
- 3 *Science and Technology* **2002,** *37* (8), 1851-1860, DOI: 10.1081/SS-120003047.
- 4 (5) Mouedhen, G.; Feki, M.; Wery, M. D. P.; Ayedi, H. F. Behavior of Aluminum Electrodes in
- 5 Electrocoagulation Process. Journal of Hazardous Materials 2008, 150 (1), 124-135, DOI:
- 6 https://doi.org/10.1016/j.jhazmat.2007.04.090.
- 7 (6) Rusova, N.; Astashkina, O.; Lysenko, A. Adsorption of Heavy Metals by Activated Carbon
- 8 Fibres. Fibre Chemistry **2015**, 47 (4), 320-323, DOI: 10.1007/s10692-016-9687-4.
- 9 (7) Esalah Jamaleddin, O.; Weber Martin, E.; Vera Juan, H. Removal of Lead, Cadmium and Zinc
- from Aqueous Solutions by Precipitation with Sodium Di-(N-Octyl) Phosphinate. *The Canadian*
- 11 *Journal of Chemical Engineering* **2010,** 78 (5), 948-954, DOI: 10.1002/cjce.5450780512.
- 12 (8) Ojovan, M. I.; Lee, W. E. Chapter 14 Treatment of Radioactive Wastes. In *An Introduction*
- to Nuclear Waste Immobilisation; Ojovan, M. I.; Lee, W. E., Eds.; Elsevier: Oxford, 2005; pp 149-
- 14 178.
- 15 (9) Pal, P. Chapter 2 Chemical Treatment Technology. In *Industrial Water Treatment Process*
- 16 *Technology*; Pal, P., Ed.; Butterworth-Heinemann: 2017; pp 21-63.
- 17 (10) Madadrang, C. J.; Kim, H. Y.; Gao, G.; Wang, N.; Zhu, J.; Feng, H.; Gorring, M.; Kasner, M.
- L.; Hou, S. Adsorption Behavior of Edta-Graphene Oxide for Pb (Ii) Removal. ACS Applied
- 19 *Materials & Interfaces* **2012**, *4* (3), 1186-1193, DOI: 10.1021/am201645g.
- 20 (11) Ramesha, G. K.; Sampath, S. In-Situ Formation of Graphene–Lead Oxide Composite and Its
- 21 Use in Trace Arsenic Detection. Sensors and Actuators B: Chemical 2011, 160 (1), 306-311, DOI:
- 22 https://doi.org/10.1016/j.snb.2011.07.053.

- 1 (12) Novoselov, K. S.; Geim, A. K.; Morozov, S. V.; Jiang, D.; Zhang, Y.; Dubonos, S. V.;
- 2 Grigorieva, I. V.; Firsov, A. A. Electric Field Effect in Atomically Thin Carbon Films. Science
- **2004,** *306* (5696), 666.
- 4 (13) Kuila, T.; Bose, S.; Mishra, A. K.; Khanra, P.; Kim, N. H.; Lee, J. H. Chemical
- 5 Functionalization of Graphene and Its Applications. *Progress in Materials Science* **2012**, *57* (7),
- 6 1061-1105, DOI: https://doi.org/10.1016/j.pmatsci.2012.03.002.
- 7 (14) Park, S.; Ruoff, R. S. Chemical Methods for the Production of Graphenes. Nature
- 8 *Nanotechnology* **2009**, *4*, 217, DOI: 10.1038/nnano.2009.58.
- 9 (15) Cao, B.; Ansari, A.; Yi, X.; Rodrigues, D. F.; Hu, Y. Gypsum Scale Formation on Graphene
- Oxide Modified Reverse Osmosis Membrane. *Journal of Membrane Science* **2018**, *552*, 132-143,
- DOI: https://doi.org/10.1016/j.memsci.2018.02.005.
- 12 (16) Grande Carlos, D.; Mangadlao, J.; Fan, J.; De Leon, A.; Delgado-Ospina, J.; Rojas Juan, G.;
- Rodrigues Debora, F.; Advincula, R. Chitosan Cross-Linked Graphene Oxide Nanocomposite
- 14 Films with Antimicrobial Activity for Application in Food Industry. *Macromolecular Symposia*
- 2017, 374 (1), 1600114, DOI: 10.1002/masy.201600114.
- 16 (17) Nguyen, H. N.; Rodrigues, D. F. Chronic Toxicity of Graphene and Graphene Oxide in
- 17 Sequencing Batch Bioreactors: A Comparative Investigation. *Journal of Hazardous Materials*
- **2018**, *343*, 200-207, DOI: https://doi.org/10.1016/j.jhazmat.2017.09.032.
- 19 (18) Akhavan, O.; Ghaderi, E. Photocatalytic Reduction of Graphene Oxide Nanosheets on Tio2
- 20 Thin Film for Photoinactivation of Bacteria in Solar Light Irradiation. *The Journal of Physical*
- 21 *Chemistry C* **2009**, *113* (47), 20214-20220, DOI: 10.1021/jp906325q.

- 1 (19) Ahmed, F.; Rodrigues, D. F. Investigation of Acute Effects of Graphene Oxide on Wastewater
- 2 Microbial Community: A Case Study. *Journal of Hazardous Materials* **2013**, *256-257*, 33-39,
- 3 DOI: https://doi.org/10.1016/j.jhazmat.2013.03.064.
- 4 (20) Smith, S. C.; Rodrigues, D. F. Carbon-Based Nanomaterials for Removal of Chemical and
- 5 Biological Contaminants from Water: A Review of Mechanisms and Applications. *Carbon* **2015**,
- 6 91, 122-143, DOI: https://doi.org/10.1016/j.carbon.2015.04.043.
- 7 (21) Perez, J. V. D.; Nadres, E. T.; Nguyen, H. N.; Dalida, M. L. P.; Rodrigues, D. F. Response
- 8 Surface Methodology as a Powerful Tool to Optimize the Synthesis of Polymer-Based Graphene
- 9 Oxide Nanocomposites for Simultaneous Removal of Cationic and Anionic Heavy Metal
- 10 Contaminants. RSC Advances **2017**, 7 (30), 18480-18490, DOI: 10.1039/C7RA00750G.
- 11 (22) Deng, S.; Upadhyayula, V. K. K.; Smith, G. B.; Mitchell, M. C. Adsorption Equilibrium and
- 12 Kinetics of Microorganisms on Single-Wall Carbon Nanotubes. *IEEE Sensors Journal* **2008**, 8 (6),
- 13 954-962.
- 14 (23) Kuilla, T.; Bhadra, S.; Yao, D.; Kim, N. H.; Bose, S.; Lee, J. H. Recent Advances in Graphene
- Based Polymer Composites. Progress in Polymer Science 2010, 35 (11), 1350-1375, DOI:
- 16 https://doi.org/10.1016/j.progpolymsci.2010.07.005.
- 17 (24) Palencia, C.; Rubio, J.; Rubio, F.; Fierro, J. L. G.; Oteo, J. L. Silane Coupling Agent Structures
- on Carbon Nanofibers. Journal of Nanoscience and Nanotechnology 2011, 11 (5), 4142-4152,
- 19 DOI: 10.1166/jnn.2011.4147.
- 20 (25) Lin, J.; Su, B.; Sun, M.; Chen, B.; Chen, Z. Biosynthesized Iron Oxide Nanoparticles Used
- 21 for Optimized Removal of Cadmium with Response Surface Methodology. Science of The Total
- 22 Environment 2018, 627, 314-321, DOI: https://doi.org/10.1016/j.scitotenv.2018.01.170.

- 1 (26) Yirsaw, B. D.; Megharaj, M.; Chen, Z.; Naidu, R. Reduction of Hexavalent Chromium by
- 2 Green Synthesized Nano Zero Valent Iron and Process Optimization Using Response Surface
- 3 Methodology. Environmental Technology & Innovation **2016**, 5, 136-147, DOI:
- 4 https://doi.org/10.1016/j.eti.2016.01.005.
- 5 (27) Marcano, D. C.; Kosynkin, D. V.; Berlin, J. M.; Sinitskii, A.; Sun, Z.; Slesarev, A.; Alemany,
- 6 L. B.; Lu, W.; Tour, J. M. Improved Synthesis of Graphene Oxide. ACS Nano 2010, 4 (8), 4806-
- 7 4814, DOI: 10.1021/nn1006368.
- 8 (28) Kang, S.; Pinault, M.; Pfefferle, L. D.; Elimelech, M. Single-Walled Carbon Nanotubes
- 9 Exhibit Strong Antimicrobial Activity. *Langmuir* **2007**, *23*, 8670-8673.
- 10 (29) Zhu, H.; Fu, Y.; Jiang, R.; Yao, J.; Xiao, L.; Zeng, G. Optimization of Copper(Ii) Adsorption
- onto Novel Magnetic Calcium Alginate/Maghemite Hydrogel Beads Using Response Surface
- Methodology. *Industrial & Engineering Chemistry Research* **2014**, *53* (10), 4059-4066, DOI:
- 13 10.1021/ie4031677.
- 14 (30) Sarkar, M.; Majumdar, P. Application of Response Surface Methodology for Optimization of
- 15 Heavy Metal Biosorption Using Surfactant Modified Chitosan Bead. Chemical Engineering
- 16 *Journal* **2011**, *175*, 376-387, DOI: https://doi.org/10.1016/j.cej.2011.09.125.
- 17 (31) Javanbakht, V.; Ghoreishi, S. M. Application of Response Surface Methodology for
- 18 Optimization of Lead Removal from an Aqueous Solution by a Novel Superparamagnetic
- 19 Nanocomposite. Adsorption Science & Technology 2016, 35 (1-2), 241-260, DOI:
- 20 10.1177/0263617416674474.
- 21 (32) Deng, S.; Ting, Y. P. Polyethylenimine-Modified Fungal Biomass as a High-Capacity
- 22 Biosorbent for Cr(Vi) Anions: Sorption Capacity and Uptake Mechanisms. *Environmental*
- 23 Science & Technology **2005**, *39* (21), 8490-8496, DOI: 10.1021/es050697u.

- 1 (33) Qiu, B.; Guo, J.; Zhang, X.; Sun, D.; Gu, H.; Wang, Q.; Wang, H.; Wang, X.; Zhang, X.;
- 2 Weeks, B. L.; Guo, Z.; Wei, S. Polyethylenimine Facilitated Ethyl Cellulose for Hexavalent
- 3 Chromium Removal with a Wide Ph Range. ACS Applied Materials & Interfaces 2014, 6 (22),
- 4 19816-19824, DOI: 10.1021/am505170j.
- 5 (34) Wang, K.; Zhang, X.; Zhang, X.; Yang, B.; Li, Z.; Zhang, Q.; Huang, Z.; Wei, Y. One-Pot
- 6 Preparation of Cross-Linked Amphiphilic Fluorescent Polymer Based on Aggregation Induced
- 7 Emission Dyes. Colloids and Surfaces B: Biointerfaces 2015, 126, 273-279, DOI:
- 8 https://doi.org/10.1016/j.colsurfb.2014.12.025.
- 9 (35) Lakard, S.; Herlem, G.; Lakard, B.; Fahys, B. Theoretical Study of the Vibrational Spectra of
- 10 Polyethylenimine and Polypropylenimine. Journal of Molecular Structure: THEOCHEM 2004,
- 11 685 (1), 83-87, DOI: https://doi.org/10.1016/j.theochem.2004.06.042.
- 12 (36) Li, N.; Bai, R. A Novel Amine-Shielded Surface Cross-Linking of Chitosan Hydrogel Beads
- for Enhanced Metal Adsorption Performance. *Industrial & Engineering Chemistry Research* **2005**,
- 14 44 (17), 6692-6700, DOI: 10.1021/ie050145k.
- 15 (37) Gong, Y.; Li, D.; Fu, Q.; Pan, C. Influence of Graphene Microstructures on Electrochemical
- Performance for Supercapacitors. *Progress in Natural Science: Materials International* **2015,** 25
- 17 (5), 379-385, DOI: https://doi.org/10.1016/j.pnsc.2015.10.004.
- 18 (38) Benoit, D. N.; Zhu, H.; Lilierose, M. H.; Verm, R. A.; Ali, N.; Morrison, A. N.; Fortner, J.
- 19 D.; Avendano, C.; Colvin, V. L. Measuring the Grafting Density of Nanoparticles in Solution by
- 20 Analytical Ultracentrifugation and Total Organic Carbon Analysis. *Analytical Chemistry* **2012,** 84
- 21 (21), 9238-9245, DOI: 10.1021/ac301980a.
- 22 (39) Chen, Y.; An, D.; Sun, S.; Gao, J.; Qian, L. Reduction and Removal of Chromium Vi in Water
- 23 by Powdered Activated Carbon. *Materials* **2018**, *11* (2), DOI: 10.3390/ma11020269.